The Structure and Magnetic Properties of Bulk Amorphous FeCoYB Alloys

KATARZYNA BLOCH*, MATEUSZ TALAR

Institute of Physics, Faculty of Production Engineering and Materials Technology, Czestochowa University of Technology, 19 Armii Krajowej Str., 42-200 Czêstochowa, Poland

In this paper the results of the structure and magnetic studies for bulk amorphous $Fe_{62}Co_{10}Y_8B_{20}$ and $Fe_{64}Co_{10}Y_6B_{20}$ alloys were presented. For the structural investigation was performed by X-ray diffractometry. It was found that investigated samples were amorphous in the as-cast state. Using a vibrating sample magnetometer (VSM) the magnetisation within magnetic fields ranging from 0 to 2T was measured. On the basis of these investigations the saturation magnetization value and the coercive field were determined. Basing on initial magnetization curve analysis in the area of so-called approach to ferromagnetic saturation, the type of structural defects having influence on magnetization in high magnetic fields were determined.

Keywords: bulk alloys, amorphous structure, Mossbauer spectroscopy, structural defects, Holstein-Primakoff paraprocess

Ferromagnetic amorphous alloys are a group of materials characterized by a lack of long range ordering of the atoms [1-5]. However, taking into account particular atoms, they can be found in the order of near and intermediate range, occurring at distances comparable with interatomic distances. Amorphous materials have structural fluctuations that lead to defects in their structure, such as free volumes [6-7].

These defects play a similar role as point defects in crystalline materials. Due to the fact that atoms of various diameters exist in amorphous alloys, structural defects depend clearly on their chemical composition [8-19]. The technique of rapid solidification of the melt causes freezing in the amorphous structure of randomly distributed free volumes. Due to the fact that the configuration of these defects is unstable, already in the process of rapid solidification a partial relaxation of the material takes place, i.e. there is a migration of defects and the merging of free volumes into larger clusters. Three dimensional clusters of free volumes are not stable and break down. In this way, linear defects are created, called pseudo-lockdown dipoles [11-12].

Structural defects occurring in amorphous materials, i.e. free volumes (point defects) and pseudo-dislocation dipoles, are sources of near and medium range stresses [20]. As a result of magnetoelastic interactions between these stresses and magnetization there is a non-collinear magnetic structure. MS magnetization of the amorphous alloy in strong magnetic fields H, can be described by the equation called the law of achieving the state of ferromagnetic saturation [21-23]:

$$\mu_0 M(H) = \mu_0 M_s \left(1 - \sum_{n=1}^{4} a_{n/2} \Big/ \mu_0 H^{n/2}\right) + \chi\mu_0 H + b(\mu_0 H)^{1/2} \quad (1)$$

where:, μ_o- magnetic permeability of the vacuum, M_S- saturation magnetization, $a_{n/2}/\mu_o H^{n/2}$ - part resulting from structural defects; n=1- for point defects, n=2 or n=4- for linear defects, $\chi\mu_o H$- a word resulting from the paramagnetism of electrons in the band and diamagnetism of closed shells in atoms, $b(\mu_o H)^{1/2}$ - determines the increase in magnetization due to the suppression of spin waves by the magnetic field.

The aim of the work was to examine the structure and magnetic properties, i.e. magnetization of saturation and coercivity field of the massive alloy $Fe_{62}Co_{10}Y_8B_{20}$. The aim was also to determine the type of defects occurring in the examined material and to determine their impact on the magnetization process, using the theory of H. Kronmuller.

Computational details

A massive amorphous $Fe_{62}Co_{10}Y_8B_{20}$ alloy was used for the investigations. The alloy ingots were obtained by melting the alloy components in the arc under argon atmosphere. The element boron was added to the alloy in the form of FeB alloy. Amorphous rods 2 cm long and 1 mm in diameter were obtained by the injection-suction method. To avoid oxidation of the samples, they were also produced in an argon atmosphere.

The structure of the samples was investigated by means of a Bruker D8 Advance X-ray diffractometer, equipped with a CuK_α lamp. The investigations were performed over the 2Θ range, from 30° to 120°, using a measurement step of 0.02° and time was 5s per step.

The structure of obtained alloys was also studied using Mossbauer spectroscopy on POLON equipment. Those measurements employed Mossbauer source ^{57}Co. Using NORMOS software for Mossbauer spectra analysis allowed to obtain distributions of hyperfine fields induction at the ^{57}Fe nuclei.

The hysteresis loops and magnetization curves as a function of the strenght of the magnetizing field were recorded by a vibrating sample magnetometer.

Analyzing high-field magnetisation curves according to the law of approach to ferromagnetic saturation of H. Kronmüller, the type of defects present in the alloy was determined.

Results and discussions

X-ray diffraction was used to study the structure of the obtained alloys. Figures 1 and 2 present the obtained diffraction patterns for powdered alloy samples $Fe_{64}Co_{10}Y_6B_{20}$ (fig. 1) and $Fe_{62}Co_{10}Y_8B_{20}$ (fig. 2).

The obtained X-ray diffraction patterns are typical for amorphous materials. Only the wide maximum at an 2Θ angle of 45° is visible, called the amorphous hallo. In these patterns, there are no narrow maximas, characteristic of crystalline materials.

Amorphousness of the tested materials confirmed the results of the Mossbauer study. Figures 2 and 3 present the

**email: 23kasia1@wp.pl*

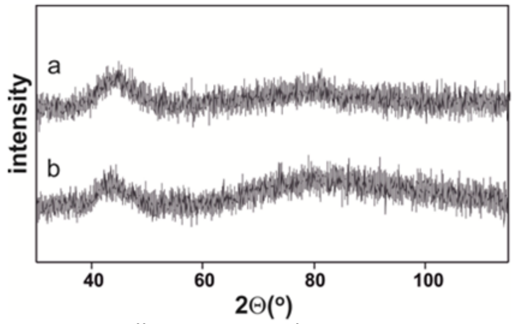

Fig. 1. X-ray diffraction pattern for powdered alloy samples: $Fe_{64}Co_{10}Y_6B_{20}$ (a) and $Fe_{62}Co_{10}Y_8B_{20}$ (b)

Mossbauer transmission spectra (fig. 2a, c) and the hyperfine field distributions obtained from them (Fig. 2b, d) for studied alloys.

The Mossbauer transmission spectra recorded for the alloys consist of Zeeman sextets with wide overlapping lines, which is characteristic of the ferromagnetic amorphous materials. There is also a slight asymmetry of the lines in these sextet, which according to Le Caër and Dubois [24] it is caused mainly by the anisotropy of the hyperfine field in the alloy. Obtained for the alloys distributions of hyperfine field induction are asymmetrical and three components can be distinguished, which indicates the presence of areas with different concentrations of iron in the sample [25].

The value of the average hyperfine field induction is 22.77 T for alloy $Fe_{64}Co_{10}Y_6B_{20}$ and 22.56 T for $Fe_{62}Co_{10}Y_8B_{20}$. The higher value of this parameter indicates the higher bulk density of the atoms in the sample comprising of 6%at. of yttrium.

Tests of magnetic properties in strong magnetic fields were carried out using a vibration magnetometer. Static hysteresis loops measured for the tested materials are shown in figure 3.

The static hysteresis loops obtained for the tested alloys have a typical shape as for soft magnetic materials. On the basis of these measurements, magnetization of saturation and coercive field were determined, which amount to 1.29 T and 24.66 A/m for the alloy $Fe_{64}Co_{10}Y_6B_{20}$ and 1.25 T and 38.20 A/m for $Fe_{62}Co_{10}Y_8B_{20}$. Based on the obtained results, it can be concluded that the structure of the alloy $Fe_{64}Co_{10}Y_6B_{20}$ it is more homogeneous and relaxed. This alloy is characterized by a higher magnetization value which is consistent with the results of the Mössbauer study. In addition, this alloy has a lower coercive field value. The dominant mechanism of the formation of magnetic hysteresis in amorphous materials is the inhibition of domain wall motion in local stress centers. During the production of material with less yttrium content, as a result of structural relaxation, more atoms took their locally ordered positions. This, in turn, led to a higher density of atom packing in the structure and a reduction in free volumes.

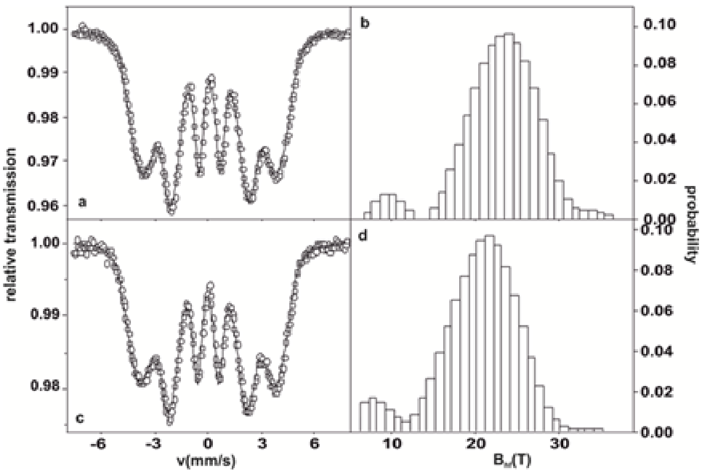

Fig. 2. Transmission Mossbauer spectra (a, c) and the corresponding hyperfine field distributions (b, d) for powdered alloy sample $Fe_{64}Co_{10}Y_6B_{20}$ (a, b) and $Fe_{62}Co_{10}Y_8B_{20}$ (c, d)

Figure 4 show the curves of the original magnetization for the investigated alloys.

The analysis of the primary magnetization curves was carried out in accordance with the theory of H. Kronmuller [7]. On the basis of the analysis of the area called approach to ferromagnetic saturation, the type of structural defects that affect the magnetization process of the obtained alloys was determined. Figures 5, 6 show the high-field magnetization curves obtained for the tested mass alloys.

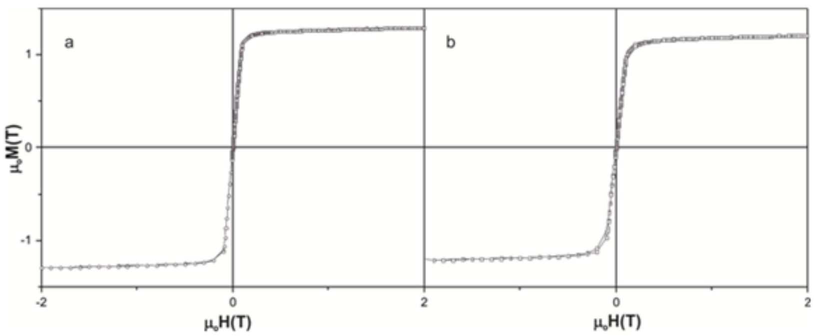

Fig. 3. Static hysteresis loop measured for the alloys: $Fe_{64}Co_{10}Y_6B_{20}$ (a) and $Fe_{62}Co_{10}Y_8B_{20}$ (b)

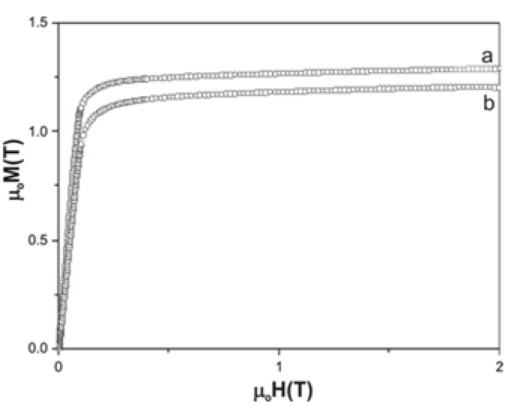

Fig. 4. The original magnetization curve for the alloys: $Fe_{64}Co_{10}Y_6B_{20}$ (a) and $Fe_{62}Co_{10}Y_8B_{20}$ (b)

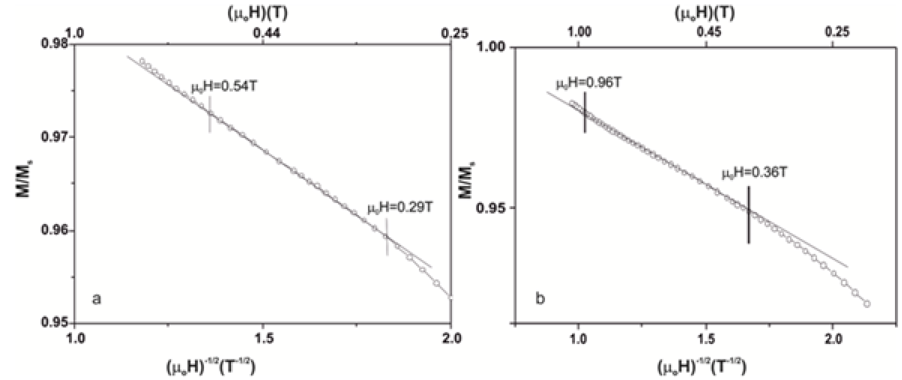

Fig. 5. High-field magnetization curve $M/M_s((\mu_0H)^{-1/2})$ for the investigated alloys: $Fe_{64}Co_{10}Y_6B_{20}$ (a) and $Fe_{62}Co_{10}Y_8B_{20}$ (b)

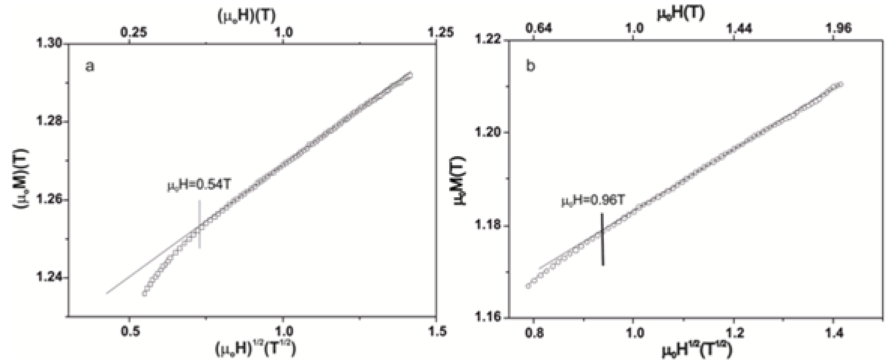

Fig. 6. Magnetization cuvre $\mu_0M_s((\mu_0H)^{1/2})$ for the investigated alloys: $Fe_{64}Co_{10}Y_6B_{20}$ (a) and $Fe_{62}Co_{10}Y_8B_{20}$ (b)

In the case of studied alloys, we observe a linear relationship of reduced magnetization (M/M_S) from magnetic field induction $(m_oH)^{-1/2}$ in field induction range. This shows that, respectively, in the fields from 0.29 T to 0.54 T for $Fe_{64}Co_{10}Y_6B_{20}$ and 0.36 T to 0.96 T for the alloy, the magnetizing process is associated with small rotations of magnetic moments near point defects. In stronger magnetic fields (>0.54 T for $Fe_{64}Co_{10}Y_6B_{20}$, >0.96 T dla $Fe_{62}Co_{10}Y_8B_{20}$) a slight increase in magnetization occurs as a result of Holstein-Primakoff paraproces (fig. 6a, b) [26]. This process is related to the suppression of thermally excited spin waves through a magnetic field.

Conclusions

As part of the work, structure, microstructure and magnetic properties were investigated for massive amorphous alloys $Fe_{64}Co_{10}Y_6B_{20}$ and $Fe_{62}Co_{10}Y_8B_{20}$. Alloy samples were obtained by pressing in the form of bars with a length of 20 mm and a diameter of 1 mm. Based on the structure tests, it was found that the tested materials in the state after solidification are amorphous alloys. Amorphous structure of alloys were confirmed by the results obtained on the basis of the Mössbauer study. Additionally, it was found that the value of the average hyperfine field induction is higher for $Fe_{64}Co_{10}Y_6B_{20}$ alloy, which indicates a higher density of atoms in this material. On the basis of magnetic tests, it was found that the obtained static hysteresis loops have a shape typical for magnetic materials exhibiting magnetically soft properties. On the basis of their analysis, saturation $Fe_{64}Co_{10}Y_6B_{20}$ magnetization and coercive field were determined. It was found that the massive amorphous alloy is characterized by a higher saturation magnetization value and a lower coercive field value. In addition, based on magnetisation studies in strong magnetic fields, it was found that the magnetization process of the investigated alloys, when there is no domain structure in them, is mainly affected by point defects. In stronger magnetic fields, in both studied alloys, the increase in magnetization occurs as a result of suppression of thermally excited spin waves by the magnetic field (Holstein-Prifmakoff paraproces).

References

1.INOUE A., GOOK J. S., Mater. Trans. JIM **36**, 1995, pp.1180-1183.

2.INOUE A., KATSUYA A., Mater. Trans. JIM **37**, 1996, pp.1332-1336.

3.INOUE A., ZHANG T., ITOI T., TAKEUCHI A., Mater. Trans. JIM **38**, 1997, pp. 359-362.

4.INOUE A., KOSHIBA H., ITOI T., MAKINO A., Appl. Phys. Lett. **73**, 1998, pp. 744-746 .

5.NABIALEK M., Arch. Metall. Mater.**61**, 2016, pp. 445-450.

6.GRUSZKA K., Materiali in Tehnologije **50** (5), 2016, pp. 707-712.

7.KRONMULLER H., J. Appl. Phys. **52**, 1981, pp.1859-1864.

8.GONDRO J., B£OCH K., NABIA£EK M., GARUS S., Materiali in tehnologije/Materials and technology **50**, 2016, pp. 559-564.

9.SZOTA M., Arch. Metall. Mater. **60** (4), 2015, pp. 3095-3100.

10.NABIALEK M., J. Alloys Comp. **642**, 2015, pp. 98-103.

11.B£OCH K.. NABIA£EK M., Acta. Phys. Pol. A **127**, 2015, pp. 413-414.

12.SOBCZYK K., ZBROSZCZYK J., NABIALEK M., OLSZEWSKI J., BR¥GIEL P., SWIERCZEK J., CIURZYNSKA W., LUKIEWSKA A., LUBAS M., SZOTA M., Arch. Metall. Mater. **53**, 2008, pp. 855-860.

13.NABIALEK, M., JEZ, B., JEZ, K., Rev. Chim.(Bucharest), **69**, no. 9, 2018, p. 2546.

14.GRUSZKA K., NABIALEK M., SZOTA M., BLOCH K., GONDRO J., PIETRUSIEWICZ P., SANDU A. V., MUSTAFA AL BAKRI A. M., WALTERS S., WALTERS K., GARUS S., DOSPIAL M., MIZERA J., Arch. Metall. Mater., **61**, nr. 2, 2016, p. 641–644

15.ACHITEI, D., GALUSCA, D.G., VIZUREANU, P., CARABET, R., CIMPOESU, N., Metalurgia International, **14**, 2009, p. 45

16.VIZUREANU, P., PERJU, M.C., GALUSCA, D.G., NEJNERU, C., AGOP, M., Metalurgia International, vol. XV, no. 12, 2010, p. 59-64.

17.TOTH, L., HARASZTI, F., KOVACS, T., European Journal of Materials Science and Engineering, **3**, no. 2, 2018, p. 98.

18.GARUS S., SZOTA M., Rev.Chim. (Bucharest), **69**, no. 3, 2018, p. 735-738

19.NEMES, O., Studia Universitatis Babes-Bolyai Chemia, **52**, no. 4, 2007, p. 175.

20.ŒWIERCZEK J., J. Magn. Magn. Mater. **322**, 2010, pp. 2696.

21.KRONMULLER H., IEEE Trans. Magn., **15**, 1979, pp. 1218-1225.

22.KRONMULLER H., ULNER J., J. Magn. Magn. Mater. **6**, 1977, pp. 52-56.

23.KRONMULLER H., J. Appl. Phys. **52**, 1981, pp. 1859.

24.LE CAER G., M. DUBOIS J., Physica Status Solidi (a) **64**, 1981, pp. 275-282

Manuscript received: 16.06.2018